



## 23 ABSTRACT

24 The adsorption on silica surface of polyaromatic compounds: N-(1-hexylheptyl)-N'-(5-  
25 carboxylicpentyl)-perylene-3,4,9,10-tetracarboxylic bisimide (C5Pe), N-(1-undecyl-dodecyl)-  
26 N'-(5-carboxylicpentyl)-perylene-3,4,9,10-tetracarboxylic bisimide (C5PeC11) individually  
27 and their binary mixture in heptol (mixture of heptane and toluene) solutions was studied by  
28 molecular dynamics (MD) simulation, Quartz Crystal Microbalance with Dissipation (QCM-  
29 D) and Atomic Force Microscopy (AFM). The MD simulation results showed that C5Pe  
30 molecules tend to aggregate and form a large cluster rapidly in the oil phase, reducing the  
31 energy of the system. In contrast, C5PeC11 molecules with high solubility tend to disperse in  
32 the system. As a result, more C5PeC11 molecules exhibited a stronger adsorption than C5Pe  
33 molecules on silica surfaces. In the binary mixture system, the overall solubility is only slightly  
34 lower than that in the C5PeC11 system due to the association of C5Pe with C5PeC11 molecules  
35 through  $\pi$ - $\pi$  stacking and T-stacking interactions, leading to more polyaromatic compounds  
36 available for adsorption onto silica surfaces. The enhanced adsorption of both polyaromatic  
37 compounds on silica surfaces clearly illustrates the synergy of adsorption in the mixed systems  
38 of C5Pe and C5PeC11 than the systems of their individual species. The adsorption  
39 characteristics revealed in MD simulations were confirmed by QCM-D measurement and AFM  
40 imaging. The observed synergy of adsorption provides insights into the molecular assembly at  
41 silica-oil interfaces for the fabrication of devices or sheds lights on petroleum processing.

42

## 43 ■ INTRODUCTION

44 Polyaromatic compounds such as perylene bisimide (PBI) derivatives, possess large  $\pi$ -  
45 conjugated rings, which makes these molecules owning favorable physical and chemical  
46 properties as well as special functions. It has been widely researched in the fields of material  
47 science, supramolecular assembly, biology, photochemistry, analytical chemistry and so on. The  
48 self-assembly of  $\pi$ -conjugated organic molecules has always been an active research topic, due  
49 to the high thermal stability and photostability at ambient conditions, which make it feasible for  
50 the application in optoelectronic devices. The property of easy chemical modification by  
51 various functional groups promotes the formation of well-defined nanostructures fabricated by  
52 PBIs, and inspires the research on self-assembly of n-type organic semiconductor molecules.<sup>1-</sup>  
53 <sup>2</sup> As a result, more and more efforts have been dedicated to expanding the possible applications  
54 of PBIs.<sup>3-4</sup>

55 Asphaltenes are the most aromatic of the largest, densest and heaviest components with  
56 remarkable surface-active properties in crude oil. They are defined as a solubility class, not by  
57 their structure, i.e., insoluble in alkanes such as pentane or heptane, but soluble in aromatic  
58 solvents such as toluene or xylene.<sup>5-7</sup> Such practical definition of asphaltenes means that the  
59 exact molecular structures of asphaltenes are still unknown. Asphaltenes are not a  
60 homogeneous fraction, but a mixture of molecules of fused polyaromatic rings with polar  
61 groups, branches and tails of variable lengths. The complexity and unknown molecular  
62 structure of asphaltenes make the understanding of their properties difficult. Archipelago model

63 and island model have been the recognized structure models of asphaltene molecules till now.<sup>8-</sup>  
64 <sup>10</sup> Therefore, **developing** and **studying** the model compounds with well-defined structure and  
65 properties similar to crude oil asphaltenes appear to be an excellent strategy for researchers.<sup>11</sup>  
66 Sjöblom's group designed and synthesized a series of model compounds of asphaltenes. **These**  
67 model compounds are derivatives of perylene imide molecules with branched alkyl chains and  
68 polar groups attached to the polyaromatic core.<sup>12-15</sup> Great efforts have been made to understand  
69 interfacial behaviors of these model compounds.<sup>16-19</sup>

70 As well documented, asphaltene adsorption at solid-oil interfaces is an ubiquitous phenomenon,  
71 which results in altering the wettability of solid surfaces, thus causing lots of problems in  
72 industry, such as production, transportation, petroleum refining and environmental treatment.<sup>9</sup>  
73 The adsorption of asphaltenes at liquid-solid interfaces has been studied in a wide range of  
74 systems, in order to develop the removal strategies of asphaltenes.<sup>20-22</sup> Adams reviewed the  
75 different adsorption systems. Asphaltene adsorption was determined to be a multifaceted  
76 process and sensitive to many system variables such as source and concentration of asphaltenes,  
77 physical aspects of sorbents, type of solvents, properties of rock surfaces, etc.<sup>7</sup> The adsorption  
78 of polyaromatic asphaltenes onto solid surface has been studied extensively by experimental  
79 methods, such as depletion method, quartz crystal microbalance, photothermal surface  
80 deformation spectroscopy, and contact angle measurements.<sup>11</sup> These experiments provided a  
81 great deal of valuable information on asphaltene adsorption. However, the critical information  
82 on molecular adsorption process, orientation of molecules, binding sites on solid surfaces,  
83 interaction type of asphaltenes, the state of molecular aggregates, etc., remain unavailable.

84 Molecular dynamics (MD) simulation has been extensively used to investigate the molecular  
85 aggregation of polyaromatic compounds systems.<sup>23-25</sup> The adsorption of model compounds with  
86 charged and uncharged terminal groups were studied and the stacked polyaromatic rings were  
87 identified to be orthogonally oriented to the oil-water interface. The results are in agreement  
88 with the experiments of the perylene-based type model compounds. Lots of evidences from  
89 experiments and simulations of adsorption process showed that the perylene-based type model  
90 compounds can be successfully used to mimic asphaltenes in crude oil. Recently, the mixture  
91 of different polyaromatic compounds published by Liu in a given solvent was found to  
92 significantly reduce the apparent average nanoaggregation number, indicating the influence of  
93 interactions between polyaromatic compounds on system properties.<sup>26</sup>

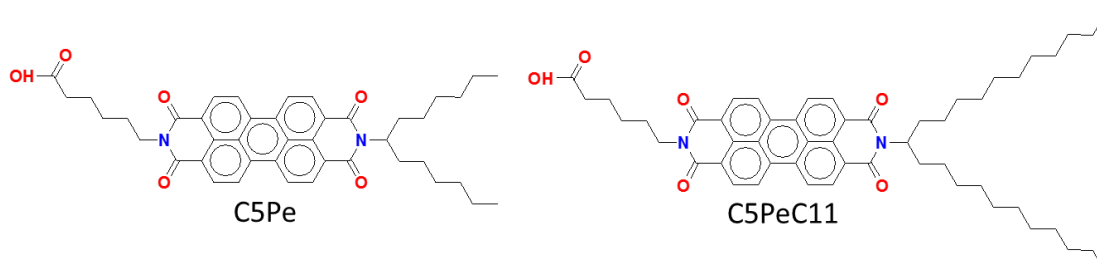
94 Other model compounds have also been investigated with MD simulation methods. Greenfiled  
95 reviewed the averaged-structure of asphaltene model compounds and the MD simulation  
96 studies.<sup>27</sup> These early studies and results provide an improved tool for relating asphalt chemical  
97 compositions to their interfacial behavior. Goual et al., for example, simulated the removal of  
98 asphaltenes from calcite mineral surfaces with surfactants and microemulsions. The results  
99 revealed that microemulsions were more effective than surfactants by swelling the oil phase.<sup>28</sup>  
100 Boek's group utilized the constraint force method to calculate the potential mean force (PMF)  
101 of asphaltene and calcite surface in vacuum, subsequently obtained the reasonable value of  
102 adsorption free energy.<sup>29</sup> Murgich et al. calculated the interaction energy of model asphaltenes  
103 and resins on neutral kaolinite surface. The results showed that van der Waals forces are the  
104 major driving force for the observed adsorption.<sup>30</sup> Increasingly, more MD simulation studies  
105 on aggregation and adsorption of polyaromatic compounds at oil-water or oil-solid interfaces

106 have been published recently.<sup>24, 31-32</sup> In summary, Boek et al. reviewed the insights and  
107 limitations of molecular dynamics simulation methods on studying asphaltene aggregation.<sup>33</sup>  
108 These authors provided a critical view on MD simulations as applied to asphaltene molecules  
109 from a number of aspects, including asphaltene structures, simulation systems and modeling,  
110 simulation details and analysis methods, etc.

111 The effect of solvent properties on adsorption of polyaromatic compounds on silica was studied  
112 in heptane and toluene.<sup>34</sup> In this work, the adsorption process and interactions of different  
113 polyaromatic compounds from organic solutions on a silica surface were investigated by  
114 molecular dynamics (MD) simulation method. The adsorption kinetics and capacities were  
115 determined by quartz crystal microbalance with dissipation (QCM-D), with molecular  
116 orientation on silica surfaces in different solvents being characterized by atomic force  
117 microscopy (AFM) imaging.

## 118 ■ SIMULATION MODELS AND METHODOLOGY

119 In this study, N-(1-hexylheptyl)-N'-(5-carboxylicpentyl)-perylene-3,4,9,10-tetracarboxylic  
120 bisimide (C5Pe) and N-(1-undecyl-dodecyl)-N'-(5-carboxylicpentyl)-perylene-3,4,9,10-  
121 tetracarboxylic bisimide (C5PeC11) (shown in Figure 1) were used as the polyaromatic  
122 compounds. The molecules both consisted of a polar terminate (carboxylic acid: -COOH) group  
123 and fused polyaromatic rings with two aliphatic chains on the other end. The difference between  
124 these two polyaromatic compounds is that C5PeC11 molecules have longer aliphatic chains  
125 than C5Pe molecules, which leads to a higher solubility in toluene. All the MD simulations  
126 were carried out using the GROMACS 5.1.4 software package with GROMOS96-53a6 united  
127 atom force field.<sup>35</sup> The details on silica slab structure and force field parameter settings are all  
128 the same as used in our previous paper.<sup>34</sup> Moreover, the optimized geometry and topology files  
129 of C5Pe and C5PeC11 were generated by Automated Topology Builder (ATB) of Repository  
130 Version 2.2.<sup>36</sup>



131

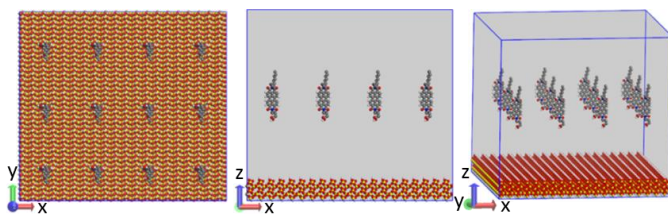
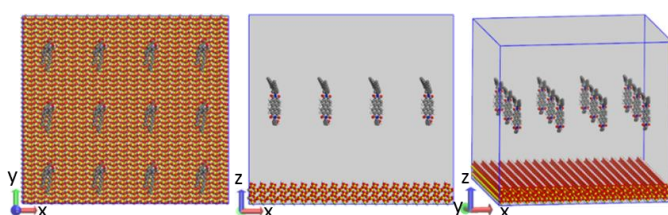
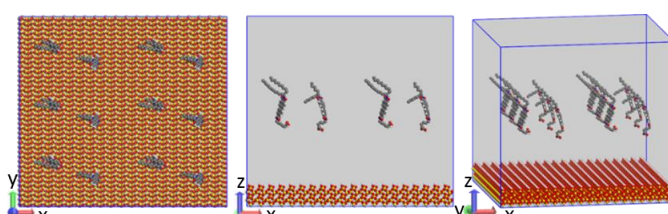
132 Figure 1. Structure of C5Pe and C5PeC11 polyaromatic compounds.

### 133 1. Configuration and Simulation Details

134 In order to investigate the adsorption of different polyaromatic compounds, it is critical to make  
135 sure that all the molecules run from the same distance to the silica surface. In this study, a box  
136 of  $10.8 \times 9.8 \times 10$  nm with a silica slab was created first. The polyaromatic compounds were  
137 arranged orderly over the surface with the distance of the closest atoms of the polyaromatic  
138 molecules being set at 3 nm away from the surface of the silica slab (shown in the inserted picture

139 in Table 1 and in the [Supporting Information](#) Figure S1). The box was then filled with heptol  
 140 (a binary mixture of equal volume of heptane and toluene). The details on the number of  
 141 molecules in box are given in Table 1.

142 Table 1. Number of molecules and molecular arrangement of initial simulation box

Molecules	Toluene	Heptane	View <sup>a</sup>
12 C5Pe	2484	1699	
12 C5PeC11	2478	1693	
6 C5Pe 6 C5PeC11	2478	1689	

143 <sup>a</sup> Colors for atoms are dark grey = C, white = H, blue = N, yellow = Si, and red = O. Heptane and toluene  
 144 solvents are not shown for clarity.

145

146 In the entire MD simulation, the periodic boundary conditions were used in x-y directions,  
 147 which made it possible for the adsorption study on only one silica-oil interface and simplified  
 148 the subsequent analysis. Other simulation processes were almost the same as used in our  
 149 previous paper.<sup>34</sup> Briefly, energy minimization was performed by the steepest descent method  
 150 and followed by the conjugate gradient method for further eliminating the steric clashes and  
 151 inappropriate geometry. The MD simulations were then performed in canonical (NVT)  
 152 ensembles at 300 K using V-rescale thermostat coupling algorithm, and continued in  
 153 isothermal–isobaric (NPT) ensembles at 300 K and 1 bar pressure using V-rescale thermostat  
 154 and Berendsen pressure coupling algorithm in the Z direction, each for 500 ps to relax the  
 155 system within the position constrain of polyaromatic compounds. The MD simulations were  
 156 continued for 100 ns in NVT ensemble with the same parameter settings used in the above NVT  
 157 simulation, but without the position constrain. During both the equilibration and production  
 158 MD simulations, leapfrog Verlet algorithm with a time step of 2 fs was used for integration of  
 159 the trajectories. The LINCS algorithm was used for all bonds, and the cutoff distance of the  
 160 neighbor list was set at 1.2 nm. The cutoff distance of 1.4 nm was adopted to calculate the L-J  
 161 potential and electrostatic interactions using particle mesh Ewald (PME) summation method.

162 The initial atomic velocities of the system were generated by Maxwell–Boltzmann distribution  
163 at the specified temperature of 300 K.

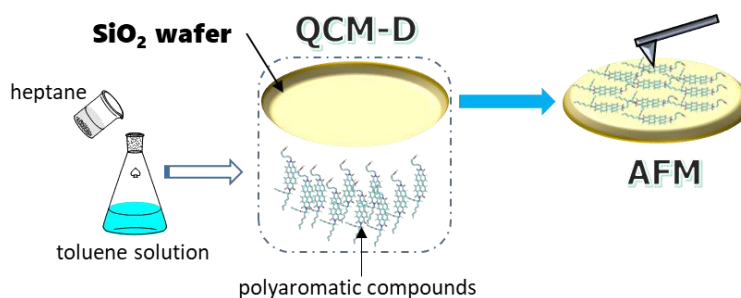
## 164 2. Experiments of QCM-D and AFM

165 The synthesis and the structural characterization of C5Pe and C5PeC11 molecules were  
166 performed in Sjöblom's group. Toluene and heptane were all of HPLC grade (Aladdin,  
167 China, >99.9%). Ethanol (Aladdin, China, 99%) and sodium dodecyl sulfate (SDS) salt  
168 (Aladdin, China, ≥99%) were used to clean the QCM crystals. All chemicals were used as  
169 received. The polyaromatic compound solutions were prepared by dissolving 0.02 g C5Pe, 0.02  
170 g C5PeC11 or the mixture of 0.01 g C5Pe and 0.01 g C5PeC11 in 20 mL of toluene under  
171 sonication for 10 min. Additional 20 mL heptane was injected into each of the three  
172 polyaromatic compounds-in-toluene solutions under sonication for 10 min before being used  
173 for the QCM-D experiments.

174 A detailed description of the QCM-D experimental protocols is available elsewhere.<sup>37</sup> Quartz  
175 Crystal Microbalance with Dissipation (QCM-D) (Q-Sense E4, Biolin Scientific, Sweden) was  
176 used in this study. The silica-coated crystals were cleaned before their use by immersing them  
177 in ethanol for 30 min, and then washed with Milli-Q water. Next, the crystals were immersed  
178 in a solution of 2% sodium dodecyl sulfate in water for 30 min, followed by washing with Milli-  
179 Q water again. For further silica hydroxylation, the above cleaned crystals were immersed in  
180 NaOH solution (about pH = 11) for 30 min followed by washing with Milli-Q water several  
181 times.<sup>34</sup> Finally, the crystals were blown dried with N<sub>2</sub>.

182 QCM-D adsorption experiments were performed with the following procedure: The machine  
183 was placed upside down in order to remove the possible effect of gravity. Heptol (equal volume  
184 of heptane and toluene) solution is initially passed through the chamber containing the crystal  
185 at 25 °C to obtain a baseline. The baseline was considered to be stable if the frequency change  
186 was less than ±1 Hz for 5 min. Three solutions of polyaromatic compounds in heptol were then  
187 injected into three separate chambers using a pump (flow rate = 500 μL/min).

188 The silica-coated crystals with polyaromatic compounds adsorbed as such were unloaded from  
189 Q-Sense E4 and blow-dried with pure nitrogen gas. Atomic force microscopy (AFM,  
190 Dimension Icon, Bruker) was used to image the morphology of the sensor surfaces in air at  
191 room temperature. Images of 10×10 μm were obtained using SCANASYST-AIR probe  
192 purchased from Bruker and Peak Force Tapping mode scan operated by ScanAsyst software.  
193 The experimental processes of QCM-D and AFM are shown in Figure 2.



194

195 Figure 2. Schematic process of QCM-D and AFM experiments

197 **1. Molecular Dynamics Simulation on Adsorption Process**

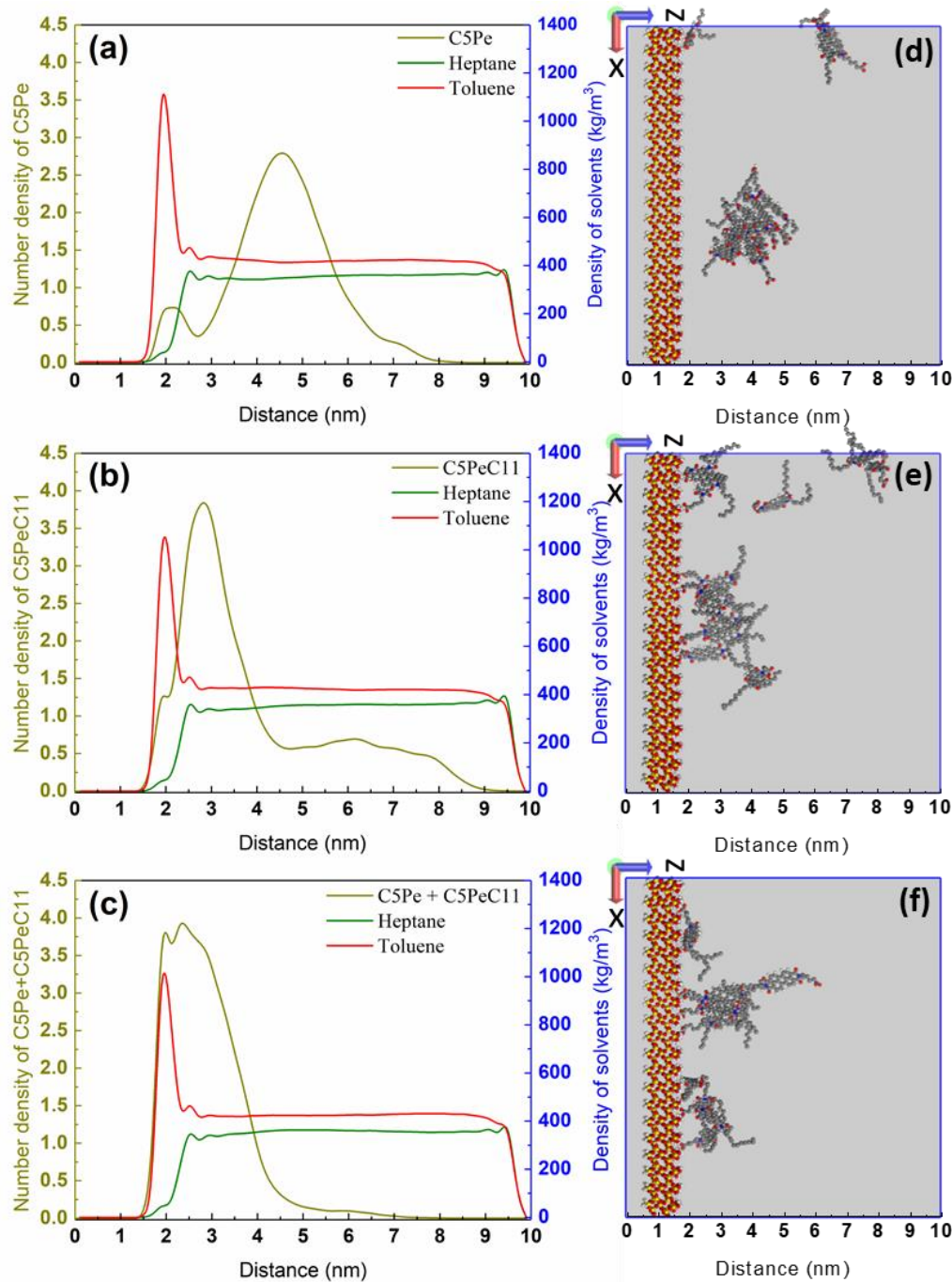
198 The number density of polyaromatic compounds and mass density profile of solvent (heptane  
199 and toluene) molecules in the systems of C5Pe, C5PeC11 or their binary mixture in heptol were  
200 analyzed along the Z-axis by taking the time average over the last 10 ns of 100 ns simulation  
201 time. For polyaromatic compounds, the distance in Figure 3 refers to the distance of COM  
202 normal to silica surfaces. The results are shown in Figure 3. Also shown in Figure 3 were  
203 snapshots of the molecular configuration on silica surfaces at 100 ns.

204 The results in Figure 3a-c showed a solvent layer of toluene adsorbed on silica surfaces with a  
205 density profile peaked at 1.8 nm, in contrast to a weak peak of heptane. Ledyastuti reported  
206 similar solvent density profiles and discussed the toluene adsorption on oil-silica interfaces in  
207 great detail.<sup>38</sup> In our study, the toluene solvent layers formed rapidly at the beginning of the  
208 simulations and were similar in all three systems, as shown in the Supporting Information  
209 Figure S2. The density profiles of toluene in Figure S2 were obtained as a time average over  
210 the first 1 ns of simulation time. The results show that the toluene adsorption layer formed long  
211 before the adsorption of polyaromatic compounds, which is shown in Figure 10 and will be  
212 discussed later.

213 Figure 3a shows a weak and broad number distribution peaks of C5Pe at  $z = 1.8$  nm and a much  
214 stronger and broader peak at  $z = 4.5$  nm. The first weak broad peak could indicate the adsorption  
215 of C5Pe as clusters as shown in the snapshot (Figure 3d). The second stronger and broader peak  
216 indicates the formation of C5Pe aggregates in bulk as also illustrated in the snapshot.

217 Compared with the C5Pe, the adsorption of C5PC11 molecules on silica in heptol is much  
218 stronger. Two distinct but overlapping peaks of C5PeC11 at  $z = 1.8$  nm and 3.1 nm were  
219 observed. The first and relatively weak peak is attributed to C5PeC11 molecules directly  
220 bonded to silica surface through interactions between polar terminate (carboxylic acid: -COOH)  
221 group of C5PeC11 and geminal silanol groups (-Si-(OH)<sub>2</sub>) on silica (shown in the Supporting  
222 Information Figure S3). The second and stronger peak located at 3.1 nm is attributed to  
223 C5PeC11 molecules associated in the form of nanoaggregates with the first layer of C5PeC11  
224 molecules firmly attached to silica surface as illustrated in the snapshot of Figure 3e. The results  
225 in Figure 3 (b and e) also show a fraction of C5PeC11 remained in the bulk solution as indicated  
226 by broad and weak distinguishable peaks at and beyond  $z = 6$  nm, mostly in the form of  
227 individual molecules or much smaller molecular aggregates.

228 For the binary mixture system, the adsorption was obviously enhanced for both C5Pe and  
229 C5PeC11 molecules as compared with the systems of individual molecule type. As shown in  
230 Figure 3 (c and f), all the molecules accumulated on silica surface with a sharp and strong peak  
231 at  $z = 1.8$  nm and a strong but board peak at  $z = 2.2$  nm, illustrating more direct binding of  
232 molecules with the silica surface in the C5Pe and C5PeC11 binary mixture system. These  
233 results indicate a strong synergy between C5Pe and C5PeC11 on promoting the adsorption of  
234 polyaromatic compounds.



235

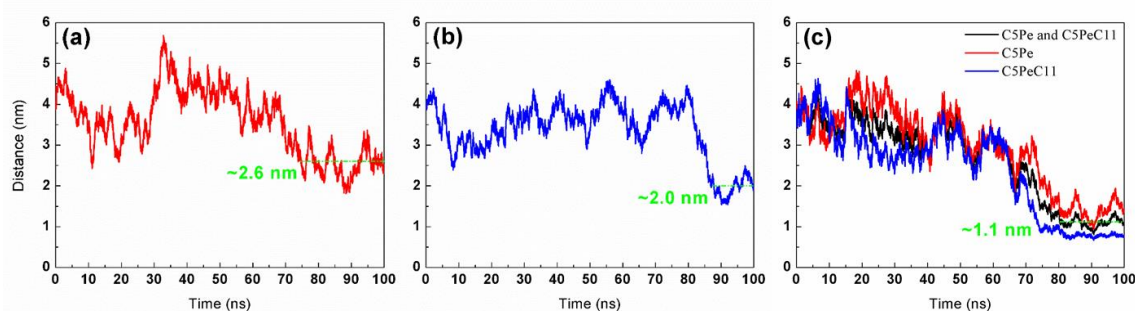
236 Figure 3. Number density of polyaromatic compounds (thick brown line) and mass density of heptane  
 237 and toluene solvents (green and red line) along the Z-axis over the last 10 ns of simulation time: (a) 12  
 238 C5Pe system, (b) 12 C5PeC11 system, and (c) 6 C5Pe and 6 C5PeC11 binary mixture system. The right  
 239 side is the snapshot of final adsorption configuration at 100 ns: (d) 12 C5Pe system, (e) 12 C5PeC11  
 240 system, and (f) 6 C5Pe and 6 C5PeC11 binary mixture system. The heptane and toluene are not shown  
 241 in the snapshots for clarity. Colors for atoms are: dark grey-C, white-H, blue-N, yellow-Si and red-O.

242

243 To gain the insights on adsorption of different polyaromatic compounds, it is more valuable to  
 244 analyze the time-dependent properties, not just the final configuration. Therefore, the  
 245 trajectories of molecules were tracked by averaging the COM (center of mass) distance of



246 molecules on the silica surface. Since the COM of C5Pe and C5PeC11 is not the same due to  
 247 the difference in the length of aliphatic chains, we considered the polyaromatic core of  
 248 polyaromatic compound without aliphatic chains to assign the COM (shown in the [Supporting](#)  
 249 [Information](#) Figure S4). The average distance between COM of polyaromatic compounds and  
 250 silica surface of three systems in heptol were shown in [Figure 4](#). The initial distance of COM  
 251 to silica surface is about 4 nm. The polyaromatic molecules are clearly seen to move close to  
 252 silica surface gradually in all systems. The final COM distance in C5Pe system fluctuated at  
 253 about 2.6 nm away from the surface. While in the C5PeC11 system, the final COM distance is  
 254 about 2.0 nm with less fluctuations, indicating a stronger binding of C5PeC11 than C5Pe on the  
 255 silica surface. The trajectories in the binary mixture system provided more important  
 256 information on the synergy effect of polyaromatic compound adsorption. The final average  
 257 COM distance of all polyaromatic compounds is at about 1.1 nm with much smaller fluctuations  
 258 (shown in [Figure 4c](#) black line), indicating a much stronger adsorption of C5Pe and C5PeC11  
 259 in the binary mixture system than that in the individual molecular species systems. More  
 260 importantly, the average COM distance of C5Pe or C5PeC11 in binary mixture system is  
 261 smaller than the average COM distance of corresponding single compound systems, shown by  
 262 red and blue profiles, respectively.



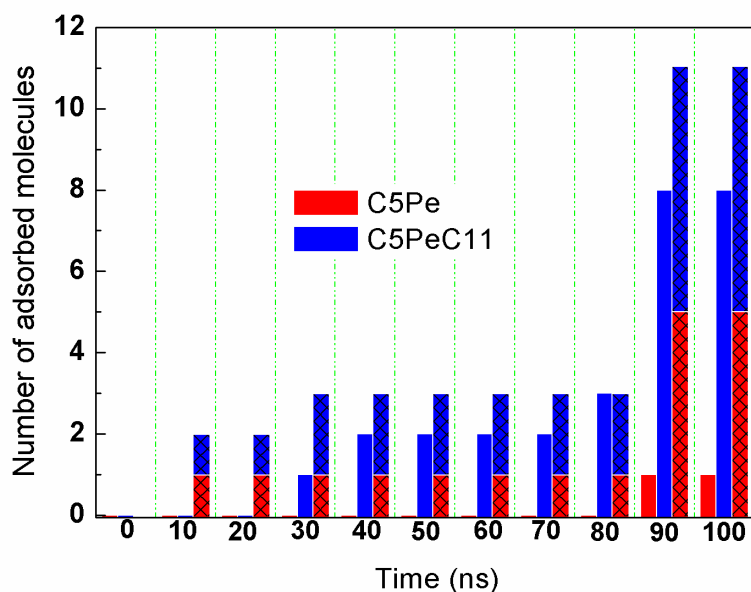
263

264 Figure 4. Average distance between COM (center of mass without aliphatic chains) of polyaromatic  
 265 compounds and silica surface in heptol as a function of time: (a) 12 C5Pe system, (b) 12 C5PeC11 system,  
 266 (c) 6 C5Pe and 6 C5PeC11 binary mixture system.

267

268 The number of molecules that adsorbed on the silica surface was analyzed at every 10 ns  
 269 intervals and the results are shown in [Figure 5](#). Here the number of polyaromatic molecules  
 270 adsorbed on silica surfaces was calculated in two steps. First, we define the cluster (aggregation of  
 271 polyaromatic compounds) using the same method published in our previous.<sup>34</sup> Briefly, the cluster  
 272 was updated whenever a molecule moved into the cut off (0.55 nm) around a molecule in the cluster,  
 273 including a single molecule as monomer. Next, we calculate the distance of the closest atom in a  
 274 cluster to the silica surface. Once the distance is less than 0.5 nm, the cluster was regarded as being  
 275 adsorbed. The number of cluster (including single molecules as adsorbed monomers) meeting this  
 276 criterion was calculated as number of molecules adsorbed. C5Pe alone showed a negligible  
 277 adsorption up to 80 ns, when only one out of 12 C5Pe molecules adsorbed. This result illustrates  
 278 a weak adsorption of C5Pe alone on silica surfaces. For C5PeC11 alone, the adsorption of a  
 279 single C5PeC11 was observed at 30 ns and increased gradually to 3 C5PeC11 molecules at 80  
 280 ns when a significant increase to 8 in the number of C5PeC11 molecules adsorbed was observed.  
 281 In contrast, the adsorption of C5PeC11 and C5Pe was observed at as early as 10 ns, indicating

282 a strong synergy of C5Pe and C5PeC11 in promoting their adsorption on silica in heptol. The  
 283 molecules adsorbed remained at 3 for an extended period with a step increase in the number of  
 284 molecules adsorbed was observed at 90 ns simulation time. Although this step increase  
 285 corresponded to the observed step increase in the C5PeC11 system, more C5Pe molecules were  
 286 shown to be adsorbed. The results on the number of the adsorbed molecules and the average  
 287 COM distance of polyaromatic molecules to silica surfaces clearly illustrate the synergy  
 288 between C5PeC11 and C5Pe on their adsorption on silica in their binary mixture system.

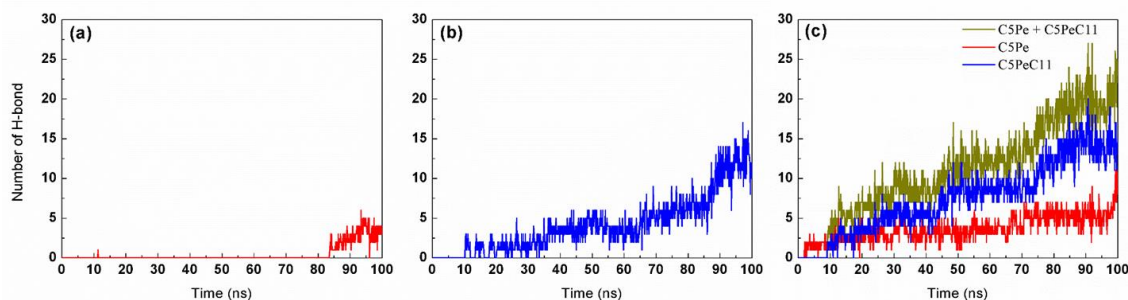


289  
 290 Figure 5. Number of molecules adsorbed on silica surfaces at different simulation time. (The stacked  
 291 columns of shaded patterns represent the binary mixture system.)  
 292

293 To better understand the observed adsorption characteristics of polyaromatic molecules on  
 294 silica surfaces in heptol, the number of hydrogen bonds **between polyaromatic molecules and**  
 295 **silica surface** was determined as a function of simulation (adsorption) time, which allows us to  
 296 elucidate when and how many molecules adsorb on silica surface. It is not surprising to see  
 297 the absence of hydrogen bonds until 84 ns for the C5Pe system (shown in Figure 6a) due to the  
 298 absence of C5Pe adsorbed on the silica as shown in Figure 5. On the contrary, polyaromatic  
 299 compounds gradually adsorb on silica surfaces after 10 ns with increasingly more hydrogen  
 300 bonds formed in the C5PeC11 system (shown in Figure 6b). In the binary mixture system, much  
 301 more hydrogen bonds were calculated compared with the individual molecular species systems,  
 302 as anticipated. In the binary system, the polyaromatic compounds adsorb rapidly on the  
 303 surface at the beginning of the simulation (shown in Figure 6c). More interestingly, the number  
 304 of hydrogen bonds **between polyaromatic molecules and silica surface** contributed by 6 C5Pe  
 305 or 6 C5PeC11 is also more than the corresponding individual molecular species systems of 12  
 306 molecules. The number of hydrogen bonds in Figure 6 clearly shows a strong and rapid  
 307 adsorption of C5Pe and C5PeC11 in the binary mixture system, which proved the synergy in  
 308 the adsorption of polyaromatic compounds.

309 In this section, the synergy effect of C5Pe and C5PeC11 is further discussed. Although the  
310 polyaromatic compounds distribution was discussed in [Figure 3](#), the results were not sufficient  
311 to explain the interactions between C5Pe and C5PeC11 molecules. The top views of the final  
312 configuration at 100 ns in the three systems are shown in [Figure 7](#), which illustrate the strong  
313 aggregation of C5Pe, followed by C5PeC11 and then C5Pe and C5PeC11 in the mixture, as  
314 anticipated.

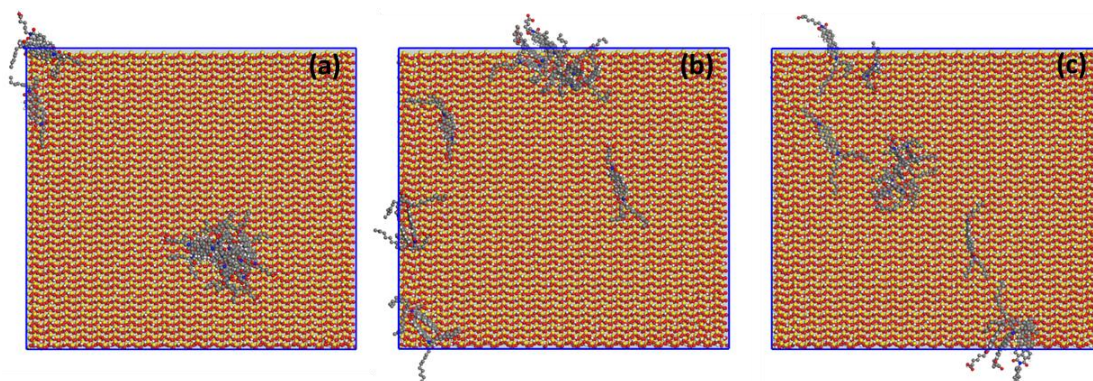
315



316

317 Figure 6. Number of hydrogen bonds **between polyaromatic molecules and silica surface** as a function  
318 of simulation time in (a) 12 C5Pe system, (b) 12 C5PeC11 system, (c) 6 C5Pe and 6 C5PeC11 binary  
319 mixture system.

320



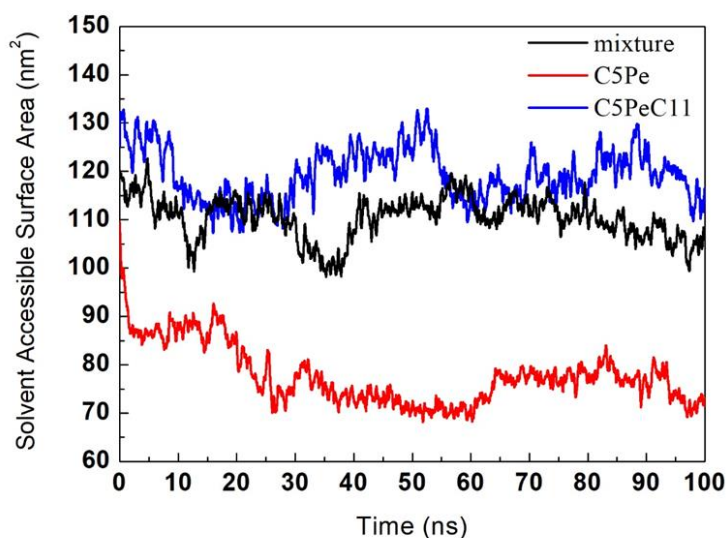
321

322 Figure 7. Top views of the final configuration at 100 ns: (a) 12 C5Pe system, (b) 12 C5PeC11 system,  
323 6 C5Pe and 6 C5PeC11 binary mixture system.

324

325 In order to explain the observed trend in molecular aggregation as a function of simulation time,  
326 the solvent accessible surface area (SASA) of polyaromatic compounds is calculated for the  
327 three systems and the results are shown in [Figure 8](#). The SASA data is a measure on the  
328 interactions of polyaromatic compounds with solvents and hence among themselves in  
329 corresponding solvents. It is clear to see a rapid reduction in the SASA of C5Pe, with the value  
330 of SASA levelled off after 25 ns and with low fluctuations. The result indicates the formation  
331 of the aggregate within 25 ns in the system (shown in the [Supporting Information](#) Figure S5).  
332 The observed low fluctuations illustrate a strong aggregation of C5Pe molecules with each other  
333 in the solvent. The free energy of the system was reduced by the aggregation of molecules,  
334 resulting in a weak adsorption of polyaromatic compounds on silica surface. In contrast, the  
335 SASA reduced slowly with high fluctuations in the C5PeC11 system, most likely due to the  
336 high solubility of C5PeC11 in heptol solvents. The solubilization of C5PeC11 increases the

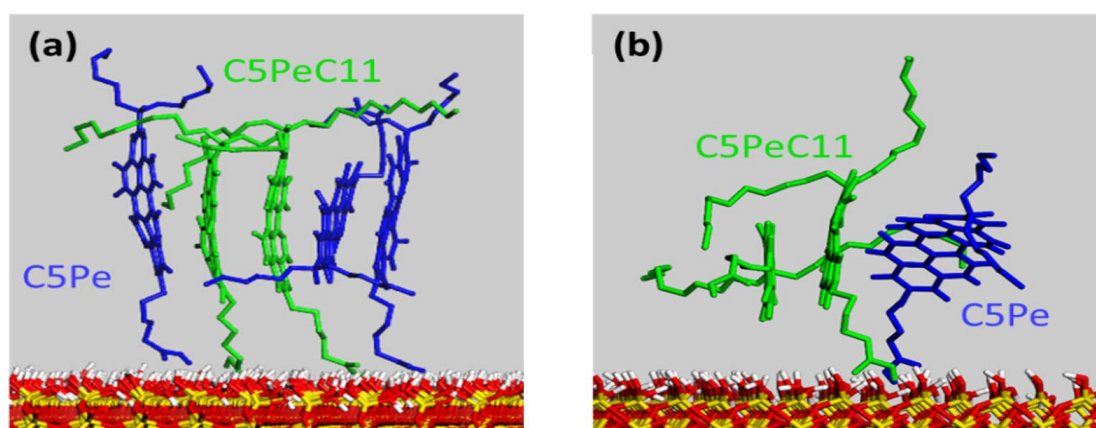
337 chance for polyaromatic compounds to adsorb on silica surface. For the binary mixture system,  
338 the SASA decreased slowly as in C5PeC11 system with the curve of SASA falling slightly  
339 below the curve for the C5PeC11 individual component system. It appears that the presence of  
340 C5PeC11 enhances the access of C5Pe by solvent molecules due to the association between  
341 C5Pe and C5PeC11. Such increase in SASA of C5Pe by C5PeC11 led to an increased  
342 adsorption of C5Pe and C5PeC11 on silica.



343  
344 Figure 8. Solvent accessible surface area of the C5Pe, C5PeC11 and their binary mixture system as a  
345 function of simulation time.

346  
347 The aggregation between C5Pe and C5PeC11 in the binary mixture system was investigated. It  
348 is interesting to find two kinds of interaction configurations on the surface: (a)  $\pi$ - $\pi$  stacking,  
349 and (b) T-stacking (shown in Figure 9). These two types of stacking between polyaromatic  
350 compounds have been reported in a number of studies.<sup>23, 39</sup>

351



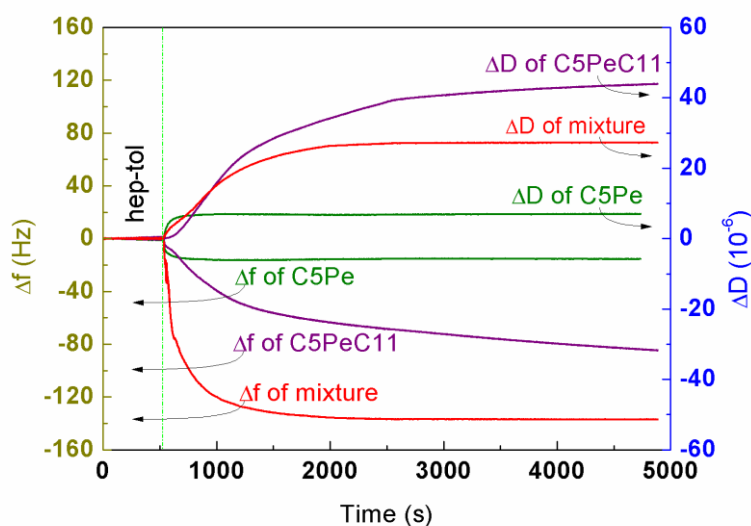
352  
353 Figure 9. Configuration of C5Pe and C5PeC11 adsorption on silica surface in a binary mixture system.  
354 (a)  $\pi$ - $\pi$  stacking, (b) T-stacking  
355

356 The  $\pi$ - $\pi$  stacking or T-stacking interaction between C5Pe and C5PeC11 in the bulk led to formation  
357 of small C5Pe-C5PeC11 clusters in the bulk. The small clusters of high diffusivity and large number  
358 binding sites exhibit more effective adsorption on silica surface than larger clusters of C5Pe (shown  
359 in the videos of [Supporting Information](#) SI-trimer and SI-pentamer). From the video, it is clear  
360 to see the trimer formed at 30 ns in bulk solvents and then adsorbed on silica surface. As for the  
361 pentamer, the situation is more complex. First, the dimer and trimer formed, respectively, in the bulk.  
362 The dimer then adsorbed after an extended simulation time. Next the interaction of the trimer from  
363 bulk solution with the dimer adsorbed led to the formation of pentamer on the silica surface and  
364 rearrangement on silica surface to the final state of adsorbed cluster (pentamer) configuration. From  
365 the final configuration at 100 ns of C5PeC11 system, the largest aggregate is dimer, while there are  
366 pentamer and trimer in the C5Pe-C5PeC11 mixture system. The steric hindrance of longer aliphatic  
367 chains impeded the aggregation of C5PeC11. The addition of C5Pe with shorter aliphatic chains  
368 provided a compromise to reduce the steric hindrance of C5PeC11 by its aggregation with C5PeC11,  
369 allowing more active polar terminals exposed for adsorption. This is the mechanism of the enhanced  
370 C5Pe adsorption in the mixed molecular system by its association with C5PeC11 molecules.  
371

## 372 2. Experiments of QCM-D

373 To confirm the significant findings by MD simulations, the **adsorption** of polyaromatic  
374 compounds either individually or in the binary mixture was studied using QCM-D method. In  
375 each experiment, heptol was injected first into the QCM-D system to establish the baseline,  
376 followed by the flow of corresponding polyaromatic compound solutions to determine the  
377 adsorption process by recording the change in the resonance frequency ( $\Delta f$ ) and dissipation  
378 ( $\Delta D$ ) of QCM-D silica sensors. [Figure 10](#) shows a rapid but small decrease (15 Hz) in the  
379 resonance frequency accompanied by a small increase in dissipation of  $8 \times 10^{-6}$  when C5Pe in  
380 heptol solution was allowed to contact with the silica sensor surfaces, indicating a limited  
381 adsorption of C5Pe molecules from its heptol solutions. A much significant decrease by 80 Hz  
382 in the resonance frequency with a significant increase in  $\Delta D$  by  $43 \times 10^{-6}$  was observed for the  
383 C5PeC11 system, indicating a much stronger adsorption of C5PeC11 than that of C5Pe on silica  
384 surfaces. **It is however surprising to see an even larger decrease in the resonance frequency by**  
385 **140 Hz, but with a much less increase in  $\Delta D$  by  $28 \times 10^{-6}$  in the binary mixture system as**  
386 **compared with the case for C5PeC11 alone.** At the same total polyaromatic compounds  
387 concentration (0.5g/L) for each system, the larger decrease in the resonance frequency indicates  
388 more molecules adsorbed on the silica sensor surfaces, which agrees with the MD simulation  
389 results in [Figure 3](#), where two strong overlapping peaks were observed in the mixed system  
390 than that in the individual component systems. More importantly, the close distances of the two  
391 peaks to the silica surface would indicate a more compact configuration of the adsorbed  
392 polyaromatic molecules, which would correspond to a smaller  $\Delta D$  increase as experimentally  
393 observed when compared with the case of C5PeC11 alone in heptol. Qualitatively, the observed  
394 decreases of  $\Delta f$ , which are in the order of C5Pe+C5PeC11 mixture > C5PeC11 > C5Pe, agreed  
395 well with the decreasing peak intensity of adsorbed polyaromatic molecules observed in MD  
396 simulations shown in [Figure 3](#). Such agreement confirms not only the synergy effect of C5Pe  
397 and C5PeC11 adsorption, but also the accuracy and the value of MD simulations. **In the current**  
398 **systems, the minimal dissipation change for C5Pe is linked with negligible adsorption of C5Pe**

399 on silica surfaces due to its low solubility in heptol, which forces molecules to form compact  
 400 aggregates in the bulk and hence the loss of their ability to bind with silica surfaces. For  
 401 C5PeC11 of high solubility in the heptol and steric hindrance from its aliphatic chains, the  
 402 aggregation of C5PeC11 in heptol is limited as such that there remain sufficient active sites  
 403 from C5PeC11 to bind with silica surfaces in floppy configurations. In the case of C5Pe and  
 404 C5PeC11 mixtures, the molecular aggregation between C5Pe and C5PeC11 is stronger than  
 405 that among C5PeC11 molecules but much weaker than that among C5Pe molecules, as shown  
 406 in our previous study with ESI-MS (Electrospray Ionization Mass Spectrometry).<sup>26</sup> Such  
 407 interactions between C5Pe and C5PeC11 accounts for the observed significant increase in  
 408 SASA of C5Pe systems that is close to the SASA value for C5PeC11 system as shown in Figure  
 409 8. Therefore, it is not surprising to see less dissipation change despite a larger change in  $\Delta f$  in  
 410 the mixed systems than that in C5PeC11 alone system.



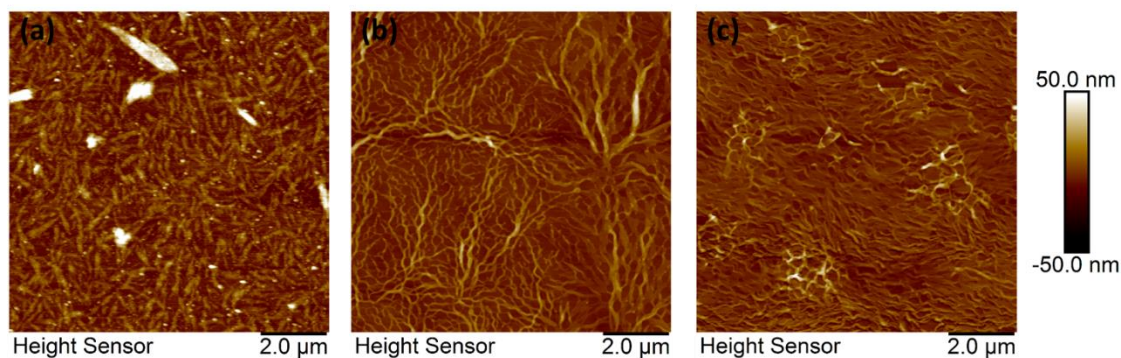
411

412 Figure 10. Frequency and dissipation shift as a function of the adsorption time in QCM-D experiments.

413

### 414 3. AFM Imaging of Adsorbed Layers

415 The silica wafers after adsorption were imaged by AFM to shed lights on the extent and the  
 416 structure of adsorbed molecules. As anticipated, the results in Figure 11a showed a clear  
 417 adsorption of C5Pe on silica in the form of aggregates with variable sizes and long strip shapes,  
 418 which were also shown in our previous work.<sup>34</sup> In the C5PeC11 system as shown in Figure 11b,  
 419 the aggregates were more compact and interconnected, in a long string of instant noodle shape.  
 420 It is the crosslinking of polyaromatic compounds that enhanced the adsorption of C5PeC11 as  
 421 compared with that of C5Pe alone. The image in Figure 11c for C5Pe and C5PeC11 binary  
 422 mixture showed a more closely packed spongy layer of polyaromatic molecules covering the  
 423 entire silica surface. This morphology of C5Pe and C5PeC11 adsorption from their binary  
 424 mixture indicated a higher adsorption capacity as observed in QCM-D measurement and MD  
 425 simulations. The results from AFM imaging confirmed the synergy adsorption of C5Pe and  
 426 C5PeC11 mixture.



427

428 Figure 11. AFM images of (a) C5Pe, (b) C5PeC11 and (c) their binary mixture adsorbed on QCM-D  
 429 silica wafer.

430

### 431 ■ CONCLUSION

432 The adsorption of individual C5Pe or C5PeC11 and their binary mixture on silica surface in  
 433 heptol solvents was investigated by molecular dynamics (MD) simulation, and further studied  
 434 by QCM-D experiments and AFM imaging. MD simulation showed a lower solubility and  
 435 stronger aggregation of short aliphatic chain C5Pe in its heptol solution as compared with the  
 436 longer aliphatic chain C5PeC11. It is therefore not surprising to see a larger aggregation in  
 437 heptol and fewer adsorptions on silica surfaces of C5Pe than C5PeC11 from corresponding  
 438 heptol solutions. It is interesting to see a clear synergy between C5Pe and C5PeC11 to enhance  
 439 their adsorption from their binary mixture system. The analysis on the trajectories of molecules  
 440 and number of hydrogen bonds revealed that the interactions of  $\pi$ - $\pi$  stacking and T-stacking  
 441 between C5Pe and C5PeC11 molecules are advantageous for not only reducing the disparity,  
 442 but also preventing rapid aggregation of polyaromatic compounds in the binary mixture system.  
 443 As a result, more C5Pe and C5PeC11 molecules adsorbed on silica surface for reducing the  
 444 system free energy. The QCM-D experiments and AFM imaging revealed a strong adsorption  
 445 and a spongy morphology of adsorbed layers on silica surface from C5Pe and C5PeC11 mixture  
 446 as compared with the cases of individual component systems, and the results were confirmed  
 447 by MD simulations. The synergetic adsorption of polyaromatic compounds revealed and  
 448 discussed in this work provides insights into the molecular assembly at silica-oil interfaces for  
 449 the fabrication of smart devices and for resolving challenges in petroleum production.

450

### 451 ■ ASSOCIATED CONTENT

452 Supporting Information

453 The Supporting Information is available and free of charge on the [ACS Publications website](#) at  
 454 DOI:

455 The detail of polyaromatic compounds arrangement in simulation box, the density  
 456 distribution of toluene in the first 1 ns along Z direction in systems, the H-bonding  
 457 interaction between polar terminate (carboxylic acid: -COOH) group and geminal  
 458 silanol groups (-Si-(OH)<sub>2</sub>), the detail of COM assigns in molecules and the snapshot of  
 459 C5Pe in system at 25 ns.

460

461 ■ AUTHOR INFORMATION

462 Corresponding Author

463 \*E-mail: [zhenghe.xu@ualberta.ca](mailto:zhenghe.xu@ualberta.ca).

464 \*E-mail: [smxu@tsinghua.edu.cn](mailto:smxu@tsinghua.edu.cn).

465

466 ORCID

467 Yong Xiong: 0000-0003-1796-6904

468 Shengming Xu: 0000-0002-6765-9251

469 Shiling Yuan: 0000-0002-4073-9470

470 Zhenghe Xu: 0000-0001-8118-1920

471

472 Notes

473 The authors declare no competing financial interest.

474

475 ■ ACKNOWLEDGMENTS

476 The financial support of the project from National Natural Science Foundation of China (Grant  
477 21333005) is greatly appreciated. Partial financial support through the Petromaks program  
478 (Norwegian Research Council) and JIP 1 (Ugelstad Laboratory) and NSERC-Industry Research  
479 Chair in Oil Sands Engineering are also gratefully acknowledged.

480

481 ■ REFERENCES

482 (1) Sun, M.; Mullen, K.; Yin, M., Water-soluble perylenediimides: design concepts and  
483 biological applications. *Chem Soc Rev* **2016**, *45*, 1513-1528.

484 (2) Balakrishnan, K.; Datar, A.; Naddo, T.; Huang, J.; Oitker, R.; Yen, M.; Zhao, J.; Zang, L.,  
485 Effect of side-chain substituents on self-assembly of perylene diimide molecules: morphology  
486 control. *J Am Chem Soc* **2006**, *128*, 7390-8.

487 (3) Chen, S.; Slattum, P.; Wang, C.; Zang, L., Self-Assembly of Perylene Imide Molecules  
488 into 1D Nanostructures: Methods, Morphologies, and Applications. *Chem Rev* **2015**, *115*,  
489 11967-98.

490 (4) Liu, L.; Sjoblom, J.; Xu, Z., Nanoaggregation of Polyaromatic Compounds Probed by  
491 Electrospray Ionization Mass Spectrometry. *Energy Fuels* **2016**, *30*, 3742-3751.

492 (5) He, L.; Lin, F.; Li, X.; Sui, H.; Xu, Z., Interfacial sciences in unconventional petroleum  
493 production: from fundamentals to applications. *Chem. Soc. Rev.* **2015**, *44*, 5446-5494.

494 (6) Mullins, O. C., The asphaltenes. *Annu. Rev. Anal. Chem.* **2011**, *4*, 393-418.

495 (7) Adams, J. J., Asphaltene Adsorption, a Literature Review. *Energy Fuels* **2014**, *28*, 2831-  
496 2856.

497 (8) Sabbah, H.; Morrow, A. L.; Pomerantz, A. E.; Zare, R. N., Evidence for Island Structures  
498 as the Dominant Architecture of Asphaltenes. *Energy Fuels* **2011**, *25*, 1597-1604.

499 (9) Chaisoontornytin, W.; Haji-Akbari, N.; Fogler, H. S.; Hoepfner, M. P., Combined  
500 Asphaltene Aggregation and Deposition Investigation. *Energy Fuels* **2016**, *30*, 1979-1986.



- 501 (10) Hoepfner, M. P.; Limsakoune, V.; Chuenmeechao, V.; Maqbool, T.; Fogler, H. S., A  
502 Fundamental Study of Asphaltene Deposition. *Energy Fuels* **2013**, *27*, 725-735.
- 503 (11) Sjoblom, J.; Simon, S.; Xu, Z., Model molecules mimicking asphaltenes. *Adv. Colloid*  
504 *Interface Sci.* **2015**, *218*, 1-16.
- 505 (12) Nordgard, E. L.; Landsem, E.; Sjoblom, J., Langmuir films of asphaltene model  
506 compounds and their fluorescent properties. *Langmuir* **2008**, *24*, 8742-51.
- 507 (13) Nordgård, E. L. k.; Sjöblom, J., Model Compounds for Asphaltenes and C80Isoprenoid  
508 Tetraacids. Part I: Synthesis and Interfacial Activities. *J. Dispersion Sci. Technol.* **2008**, *29*,  
509 1114-1122.
- 510 (14) Nordgård, E. L.; Magnusson, H.; Hanneseth, A.-M. D.; Sjöblom, J., Model compounds for  
511 C80 isoprenoid tetraacids. *Colloid Surf., A* **2009**, *340*, 99-108.
- 512 (15) Nordgard, E. L.; Sorland, G.; Sjoblom, J., Behavior of asphaltene model compounds at  
513 w/o interfaces. *Langmuir* **2010**, *26*, 2352-60.
- 514 (16) Wang, J.; Lu, Q.; Harbottle, D.; Sjoblom, J.; Xu, Z.; Zeng, H., Molecular interactions of a  
515 polyaromatic surfactant C5Pe in aqueous solutions studied by a surface forces apparatus. *J.*  
516 *Phys. Chem. B* **2012**, *116*, 11187-96.
- 517 (17) Wang, J.; van der Tuuk Opedal, N.; Lu, Q.; Xu, Z.; Zeng, H.; Sjöblom, J., Probing  
518 Molecular Interactions of an Asphaltene Model Compound in Organic Solvents Using a Surface  
519 Forces Apparatus (SFA). *Energy Fuels* **2012**, *26*, 2591-2599.
- 520 (18) Bi, J.; Yang, F.; Harbottle, D.; Pensini, E.; Tchoukov, P.; Simon, S.; Sjoebloom, J.; Dabros,  
521 T.; Czarnecki, J.; Liu, Q., et al., Interfacial Layer Properties of a Polyaromatic Compound and  
522 its Role in Stabilizing Water-in-Oil Emulsions. *Langmuir* **2015**, *31*, 10382-10391.
- 523 (19) Liu, L.; Sjöblom, J.; Xu, Z., Nanoaggregation of Polyaromatic Compounds Probed by  
524 Electrospray Ionization Mass Spectrometry. *Energy Fuels* **2016**, *30*, 3742-3751.
- 525 (20) Pradilla, D.; Subramanian, S.; Simon, S.; Sjoblom, J.; Beurroies, I.; Denoyel, R.,  
526 Microcalorimetry Study of the Adsorption of Asphaltenes and Asphaltene Model Compounds  
527 at the Liquid-Solid Surface. *Langmuir* **2016**, *32*, 7294-305.
- 528 (21) Subramanian, S.; Simon, S.; Gao, B.; Sjöblom, J., Asphaltene fractionation based on  
529 adsorption onto calcium carbonate: Part 1. Characterization of sub-fractions and QCM-D  
530 measurements. *Colloid Surf., A* **2016**, *495*, 136-148.
- 531 (22) Subramanian, S.; Sorland, G. H.; Simon, S.; Xu, Z.; Sjoblom, J., Asphaltene fractionation  
532 based on adsorption onto calcium carbonate: Part 2. Self-association and aggregation properties.  
533 *Colloid Surf., A* **2017**, *514*, 79-90.
- 534 (23) Gao, F.; Xu, Z.; Liu, G.; Yuan, S., Molecular Dynamics Simulation: The Behavior of  
535 Asphaltene in Crude Oil and at the Oil/Water Interface. *Energy Fuels* **2014**, *28*, 7368-7376.
- 536 (24) Lv, G.; Gao, F.; Liu, G.; Yuan, S., The properties of asphaltene at the oil-water interface:  
537 A molecular dynamics simulation. *Colloid Surf., A* **2017**, *515*, 34-40.
- 538 (25) Teklebrhan, R. B.; Ge, L.; Bhattacharjee, S.; Xu, Z.; Sjoblom, J., Initial partition and  
539 aggregation of uncharged polyaromatic molecules at the oil-water interface: a molecular  
540 dynamics simulation study. *J. Phys. Chem. B* **2014**, *118*, 1040-51.
- 541 (26) Liu, L.; Zhang, R. Y.; Wang, X.; Simon, S.; Sjoblom, J.; Xu, Z. H.; Jiang, B., Interactions  
542 of Polyaromatic Compounds. Part 1: Nanoaggregation Probed by Electrospray Ionization Mass  
543 Spectrometry and Molecular Dynamics Simulation. *Energy Fuels* **2017**, *31*, 3465-3474.
- 544 (27) Li, D. D.; Greenfield, M. L., Chemical compositions of improved model asphalt systems

545 for molecular simulations. *Fuel* **2014**, *115*, 347-356.

546 (28) Lowry, E.; Sedghi, M.; Goual, L., Molecular simulations of NAPL removal from mineral  
547 surfaces using microemulsions and surfactants. *Colloid Surf., A* **2016**, *506*, 485-494.

548 (29) Headen, T. F.; Boek, E. S., Potential of Mean Force Calculation from Molecular Dynamics  
549 Simulation of Asphaltene Molecules on a Calcite Surface†. *Energy Fuels* **2011**, *25*, 499-502.

550 (30) Murgich, J.; Rodríguez M, J.; Izquierdo, A.; Carbognani, L.; Rogel, E., Interatomic  
551 Interactions in the Adsorption of Asphaltenes and Resins on Kaolinite Calculated by Molecular  
552 Dynamics. *Energy Fuels* **1998**, *12*, 339-343.

553 (31) Jian, C.; Liu, Q.; Zeng, H.; Tang, T., Effect of Model Polycyclic Aromatic Compounds on  
554 the Coalescence of Water-in-Oil Emulsion Droplets. *J. Phys. Chem. C* **2017**, *121*, 10382-10391.

555 (32) Jian, C.; Zeng, H.; Liu, Q.; Tang, T., Probing the Adsorption of Polycyclic Aromatic  
556 Compounds onto Water Droplets Using Molecular Dynamics Simulations. *J. Phys. Chem. C*  
557 **2016**, *120*, 14170-14179.

558 (33) Headen, T. F.; Boek, E. S.; Jackson, G.; Totton, T. S.; Müller, E. A., Simulation of  
559 Asphaltene Aggregation through Molecular Dynamics: Insights and Limitations. *Energy Fuels*  
560 **2017**, *31*, 1108-1125.

561 (34) Xiong, Y.; Cao, T.; Chen, Q.; Li, Z.; Yang, Y.; Xu, S.; Yuan, S.; Sjöblom, J.; Xu, Z.,  
562 Adsorption of a Polyaromatic Compound on Silica Surfaces from Organic Solvents Studied by  
563 Molecular Dynamics Simulation and AFM Imaging. *J. Phys. Chem. C* **2017**, *121*, 5020-5028.

564 (35) Oostenbrink, C.; Villa, A.; Mark, A. E.; Van Gunsteren, W. F., A biomolecular force field  
565 based on the free enthalpy of hydration and solvation: The GROMOS force-field parameter sets  
566 53A5 and 53A6. *J. Comput. Chem.* **2004**, *25*, 1656-1676.

567 (36) Koziara, K. B.; Stroet, M.; Malde, A. K.; Mark, A. E., Testing and validation of the  
568 Automated Topology Builder (ATB) version 2.0: prediction of hydration free enthalpies. *J.*  
569 *Comput. Aided Mol. Des.* **2014**, *28*, 221-33.

570 (37) Chen, Q.; Xu, S.; Liu, Q.; Masliyah, J.; Xu, Z., QCM-D study of nanoparticle interactions.  
571 *Adv. Colloid Interface Sci.* **2016**, *233*, 94-114.

572 (38) Ledyastuti, M.; Liang, Y.; Kunieda, M.; Matsuoka, T., Asymmetric orientation of toluene  
573 molecules at oil-silica interfaces. *J Chem Phys* **2012**, *137*, 064703.

574 (39) Teklebrhan, R. B.; Ge, L.; Bhattacharjee, S.; Xu, Z.; Sjoblom, J., Probing Structure-  
575 Nanoaggregation Relations of Polyaromatic Surfactants: A Molecular Dynamics Simulation  
576 and Dynamic Light Scattering Study. *Journal of Physical Chemistry B* **2012**, *116*, 5907-5918.

577